

Determination of the Cable Span and Cable Deflection of Cable-driven Parallel Robots

Andreas Pott

*Institute for Control Engineering and Manufacturing Units, University of Stuttgart
Fraunhofer IPA, Stuttgart, e-mail: andreas.pott@isw.uni-stuttgart.de*

Abstract. In this paper, a method is proposed to compute the so-called cable span, i.e. the space occupied by the cables when the robot is moving within its workspace. As the cables are attached to a mostly fixed point on the robot frame, the shape of the cable span is a generalized cone. We present an efficient method *polar sorting* to compute the surface of this cone. Furthermore, the found geometry of the cone is employed in the design of the cable anchor points in order to dimension its deflection capabilities and to compute a suitable orientation for the installation of the mechanical unit.

Key words: cable-driven parallel robots, cable span, collision, deflection angles, design, workspace

1 Introduction

Cable-driven parallel robots possess a number of advantages such as light-weight design, huge workspace, and excellent dynamic capabilities. These features come at some costs in terms of difficult geometric design for complex tasks. For a cable robot, a number of collision problems need to be addressed. Firstly, the problem of cable-cable collision can significantly reduce the usable workspace and was extensively studied (e.g. in [6, 7, 3, 9]). A couple of robot design with so-called *cross-over configurations* are proposed that offer a large collision-free workspace [13, 5, 8]. Another problem arising from the application of cable robots is related to the possible collisions of the cables with the environment. Furthermore, the mechanical design of the cable deflection units with large deflection angles is involved and applies both to the distal end of the cable at the mobile platform and to the proximal guiding on the machine frame. The cable-environment interference as well as the design of the cable guiding are related and discussed within this paper. To the best of the authors knowledge, no model of the space occupied by the cables has been proposed in the literature beside the pose-dependent assessment of collisions mentioned in the papers above.

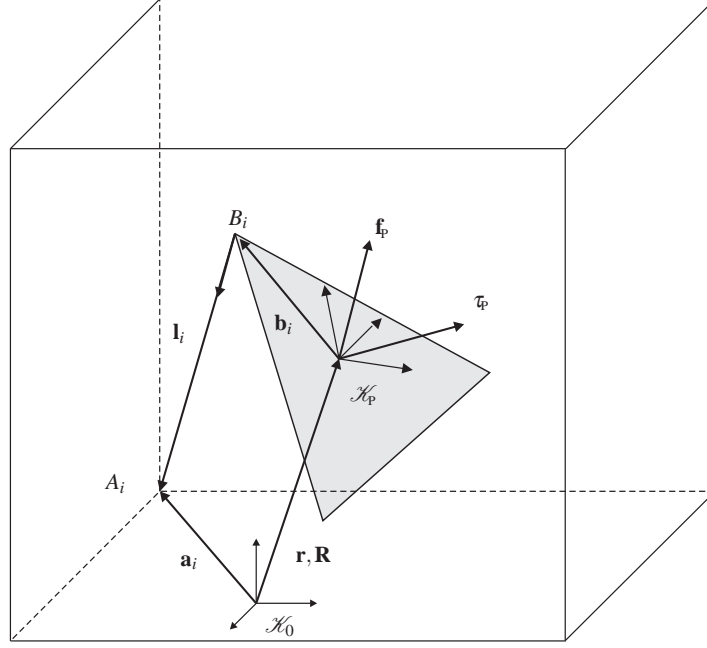


Fig. 1 Definition of the geometry and kinematics of a general cable robot

In order to deal with this problem, the *cable span* is introduced in this paper. The cable span for one cable is the space occupied by this cable while the platform travels through the robot's workspace. As shown in the remainder of this paper, the cable span is a spatial geometrical object that can be described by a generalized cone. Clearly, this region must be free of obstacles to avoid a collision with the cable. Furthermore, the cable span allows to derive the deflection requirements of the guiding pulleys in the design of the robot.

The rest of the paper is organized as follows. Sec. 2 recalls the basic kinematic and workspace issues used in this paper. In Sec. 3, some data structures for workspace computation are discussed that are essential for the computation of the cable span. Using the proposed cable span, two applications of the cable span for robot analysis and design are proposed in Sec. 4. Conclusions are closing the paper.

2 Background

The kinematic background for the cable robots is briefly reviewed for the sake of completeness. The kinematic scheme of a cable-driven parallel robot with m proximal anchor points \mathbf{a}_i and distal anchor points \mathbf{b}_i is depicted in Fig. 1. The vector \mathbf{l}_i represents the cable and it is oriented to start at the platform and point towards

the robot frame. The pose of the platform is represented by the position vector \mathbf{r} and the rotation matrix \mathbf{R} which transforms platform coordinates from the platform frame \mathcal{K}_p to world coordinates \mathcal{K}_0 . The considerations in this paper do not assume a particular parameterization of the rotation matrix, so an arbitrary parameterization can be used. The applied wrench $\mathbf{w}_p = [\mathbf{f}_p^T, \tau_p^T]^T$ is composed from the applied force \mathbf{f}_p and the applied torque τ_p . Thus, the kinematic closure equation reads

$$\mathbf{l}_i = \mathbf{a}_i - \mathbf{r} - \mathbf{R}\mathbf{b}_i, \quad i = 1, \dots, m. \quad (1)$$

As the cable span discussed in this paper is closely related to the workspace of the cable robot, a criterium needs to be considered to decide if a given pose (\mathbf{r}, \mathbf{R}) belongs to the workspace. A couple of criteria are known to account for properties such as wrench-closure [2, 4], wrench feasibility [2, 15], generation of a given wrench set [1], or absence of cable-cable interference [9]. For the procedure discussed in this paper, the kind and number of criteria is irrelevant. In the case study, we employ a simple wrench-feasibility test [12]

$$\mathbf{f}_{\min} \preceq \frac{1}{2}(\mathbf{f}_{\min} + \mathbf{f}_{\max}) - \mathbf{A}(\mathbf{r}, \mathbf{R})^{+T} \left(\mathbf{w}_p + \mathbf{A}(\mathbf{r}, \mathbf{R})^T \frac{1}{2}(\mathbf{f}_{\min} + \mathbf{f}_{\max}) \right) \preceq \mathbf{f}_{\max}, \quad (2)$$

where $\mathbf{f}_{\min}, \mathbf{f}_{\max}$ are the vectors of minimum and maximum admissible cable forces and \mathbf{A}^T is the pose-dependent structure matrix [14]. The Moore-Penrose pseudo inverse matrix of \mathbf{A}^T is denoted given by $\mathbf{A}^{+T} = \mathbf{A}(\mathbf{A}^T \mathbf{A})^{-1}$. Based on the definitions above, a pose-dependend evaluation of the workspace can be made.

3 Determination of the Cable Span

A well-known disadvantage of parallel robots and especially of cable robots is that the installation space of the robot is large compared to the workspace. One reason for this drawback is that the cables occupy a huge volume if the workspace of the robot is large. This volume that is at least temporarily taken by the cables is called *cable span* (Fig. 2). The cable span is a volumetric object for all spatial robots and a flat area like a fan for a planar robot. Based on the assumption of the standard cable model that the proximal anchor point is a pose-independent point in space, it is clear that the cable span for the i -th cable has some kind of apex at the point A_i .

3.1 Generation of relevant poses

In this paper, we assume the workspace that is assessed for the cable span is determined through discretization. In particular, we assume that the workspace is either computed by sampling a grid of positions for the translational workspace or by computing the boundary of the workspace with the hull algorithm [10].

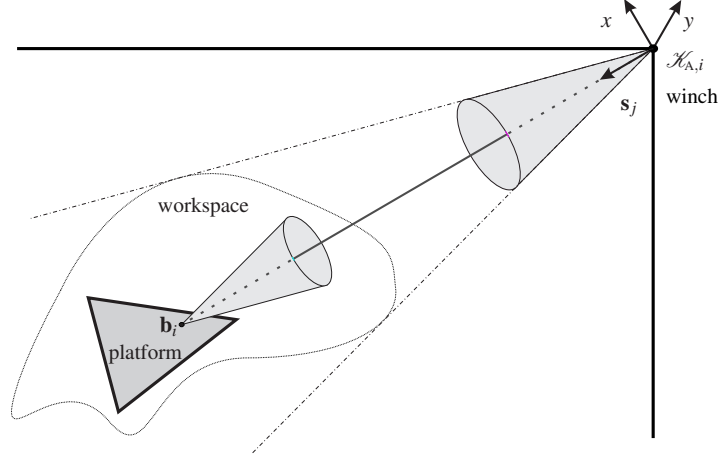


Fig. 2 Definition of the cable span based on the hull

For efficiency reasons, the workspace hull is used in the numerical study to compute the boundary of the workspace as the boundary is characteristic for the maximum cable deflections. As the surface of the workspace represents the extremal region of the workspace, the vertices of the hull include the relevant points. However, not every point on the workspace boundary is relevant for the cable span determination.

One can employ the constant orientation workspace or the total orientation workspace as basis for the determination of the cable span. For the sake of simplicity, we restrict the following considerations to the constant orientation workspace with a fixed orientation \mathbf{R}_0 of the platform and varying position \mathbf{r} . Thus, we assume the workspace \mathcal{W} to be given as a set of positions \mathbf{r}

$$\mathcal{W} = \{\mathbf{r} \in \mathbb{R}^3 \mid g(\mathbf{r}) > 0\} \quad , \quad (3)$$

where $g(\mathbf{r})$ is a function that evaluates to a positive number if the position \mathbf{r} belongs to the workspace. In this paper, Eq. (2) is used but any other workspace test can be employed instead. Respectively, one can also vary the orientation to capture the orientation workspace or the total orientation workspace. As the following consideration is purely based on efficiently sorting a set of cable vectors \mathbf{l}_i , it is straight-forward to extend the algorithm to a discretization of the orientation workspace.

Using Eq. (1), one receives for each cable i and for the k -th position \mathbf{r} in the set \mathcal{W} the respective line $\mathbf{l}_i^{(k)}$ vectors with $k = 1, \dots, N$ where N is the number of positions in the set \mathcal{W} . Geometrically speaking, this set of curves consists of line segments starting at the proximal anchor point \mathbf{a}_i and pointing towards the workspace. This set basically contains all required information about the space occupied by the cables. However, as one usually employs many points for sampling the workspace, an

estimate for a volumetrical object is sought that can be handle more efficiently than all the lines.

In the following we omit the index of the line (i) for the sake of readability and abbreviate the set of lines $\mathbf{v}_k = -\mathbf{l}_i^{(k)}$ which shall represent the common starting point at \mathbf{a}_i . Thus, a set of N points $\mathcal{V} = \{\mathbf{v}_1, \dots, \mathbf{v}_N\}$ is the input from workspace determination and the cable span shall be computed.

3.2 Sorting the line segments

Once the relevant lines from the proximal anchor point \mathbf{a}_i to the respective world coordinates of the distal anchor points $\mathbf{b}_i(\mathbf{r}, \mathbf{R})$ are determined, the structure of this bunch of lines has to be determined.

In this paper, an algorithm called *polar sorting* is proposed to extract the relevant structure from the lines. The main steps are the following

1. Determine an estimate of the cone axis
2. Construct a coordinate system located at \mathbf{a}_i with its z -axis aligned with the cone axis
3. Transform all lines \mathbf{v}_i in \mathcal{V} into this coordinate frame
4. Compute polar coordinates for the lines \mathcal{V}
5. Sort the vertices in \mathcal{V} by the azimuth angle φ
6. Cluster the vertices in n_s equal classes by intervals of the azimuth angle and approximate the enclosing cone by extracting the largest deflection angle in that interval
7. Return the surface of the generalized cone consisting of the apex at \mathbf{a}_i and the n_s characteristic vertices on its mantle of the cone

After this procedure, one has a simple triangulation with n_s triangles of the cable span that can be used in a number of applications.

3.3 Computing the Cable Span

From the structure of the workspace hull, we have an estimate used as projection center \mathbf{m} or can compute the barycenter of the workspace \mathcal{W} . If the center is unknown or a grid computation was employed, the mean value of the positions

$$\mathbf{m} = \frac{1}{N} \sum_{j=1}^N \mathbf{r}_i \quad (4)$$

is used instead. Now, the central line from \mathbf{a}_i to \mathbf{m} is employed as axis of the cone and the polar decomposition aims at sorting all the lines in the span around this central line.

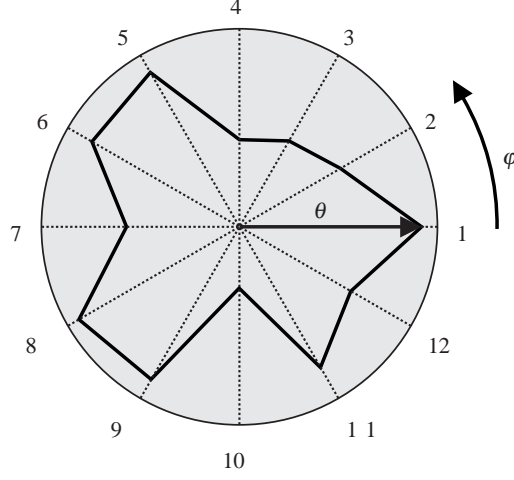


Fig. 3 Polar decomposition of the cable vector to compute the cone of the cable span for $n_s = 12$ segments

Then, a coordinate frame $\mathcal{H}_{A,i}$ is constructed at point A_i which z -axis is aligned with the (estimated) cone axis $\mathbf{e}_z = \mathbf{m} - \mathbf{a}_i$. The x -axis represented by the vector \mathbf{e}_x is perpendicular to the z -axis but has an additional degree of freedom that can be chosen arbitrarily. If a panning pulley is used for guiding the cable, it is beneficial to define the x -axis orthogonal to the first axis of the panning pulley e.g. orthogonal to the axis the pulley is panned about. The remaining y -axis is computed from the cross product $\mathbf{e}_y = \mathbf{e}_z \times \mathbf{e}_x$. The transformation matrix is then derived from the normalized vectors $(\mathbf{e}_x, \mathbf{e}_y, \mathbf{e}_z)$. This transformation is represented in terms of the transformation matrix ${}^{A,i}\mathbf{R}_0$ that maps vectors in world frame \mathcal{H}_0 to the local frame $\mathcal{H}_{A,i}$.

Based on the considerations of the workspace boundary, one can easily compute the cable span for the constant orientation workspace. The set $\mathcal{W} = (\mathbf{r}_1, \dots, \mathbf{r}_N)$ contains the N position of the workspace as introduced above. Then, one receives the world coordinates for all possible locations for the point B_i from

$$\mathbf{v}'_j = \mathbf{R}_0 \mathbf{b}_i + \mathbf{r}_j \quad \text{for } j = 1, \dots, N \quad (5)$$

which is simply a translation of the hull by \mathbf{b}_i . The cable span is approximated from connecting the point A_i with each of the vectors \mathbf{v}'_j . The resulting geometrical object is a generalized cone with a noncircular cross-section where most of the lines defined above are lying inside the cone. To normalize the representation and also to reduce the amount of data, a *polar decomposition* of the lines is proposed and described below.

The N lines of the span are distributed in n_s polar segments (Fig. 3) in the frame $\mathcal{H}_{A,i}$. Firstly, each line is transformed into the local frame $\mathcal{H}_{A,i}$ by

$${}^{A,i}\mathbf{s}_j = {}^{A,i}\mathbf{R}(\mathbf{v}'_j - \mathbf{a}_i) \quad . \quad (6)$$

Then, the spherical coordinates $\mathbf{s}_j^{(c)}$ are computed from

$$\mathbf{s}_j^{(c)} = \begin{bmatrix} r \\ \theta \\ \varphi \end{bmatrix}_j = \begin{bmatrix} \sqrt{s_x^2 + s_y^2 + s_z^2} \\ \arccos \frac{s_z}{\sqrt{s_x^2 + s_y^2 + s_z^2}} \\ \arctan 2(s_y, s_x) \end{bmatrix}_j \quad \text{with} \quad {}^A \mathbf{s}_j = [s_x, s_y, s_z]^T \quad . \quad (7)$$

These spherical coordinates $\mathbf{s}_j^{(c)}$ allow for a simple extraction of the cable span. The N line vectors are sorted in ascending order of their φ -value (Fig. 3). This sorting may effortlessly be done by storing the data in an associative container offered by most programming languages¹. Then, n_s segments of equal size are chosen for the angle φ that represent the ranges

$$\mathcal{S}_i = \left[\frac{i 2\pi}{n_s}, \frac{(i+1)2\pi}{n_s} \right]_i \quad i = 0, \dots, (n_s - 1) \quad . \quad (8)$$

Finally, one loops through the sorted list $\mathbf{s}_j^{(c)}$ of cylinder coordinates and extracts for each range \mathcal{S}_i the matching element with

$$\mathbf{s}_j^{(c)} \Big|_{\varphi \in \mathcal{S}_i} \quad (9)$$

and stores the largest angle θ for all line vectors that belong to the respective segment. After this procedure, one has a sorted list of n_s characteristic vectors of the surface of the cable span. Connecting two neighboring vectors with the apex at $\mathcal{K}_{A,i}$ gives a triangulation of the surface of the cable span. Exporting this triangulation to STL or VRML is straight forward and allows to use results within CAD systems. The list of the angles over the polar coordinate is basically a look-up table to check if a vector is inside the cone.

4 Application

In this section, a case study for determination of the cable span is presented. The case study is based on the IPAnema 1 robot geometry as given in Tab. 1. For the case studies, the translational workspace with a constant orientation of $\mathbf{R}_0 = \mathbf{I}$ is considered.

¹ The effort for this kind of sorting is $\log(N)$ for each element and it is internally done when using associative containers such as `dict` in Python or `map` in C++.

Table 1 Nominal geometric parameters in terms of base vectors \mathbf{a}_i and platform vectors \mathbf{b}_i for the IPAnema 1 robot.

cable i	base vector \mathbf{a}_i	platform vector \mathbf{b}_i
1	$[-2.0, 1.5, 2.0]^T$	$[-0.06, 0.06, 0.0]^T$
2	$[2.0, 1.5, 2.0]^T$	$[0.06, 0.06, 0.0]^T$
3	$[2.0, -1.5, 2.0]^T$	$[0.06, -0.06, 0.0]^T$
4	$[-2.0, -1.5, 2.0]^T$	$[-0.06, -0.06, 0.0]^T$
5	$[-2.0, 1.5, 0.0]^T$	$[-0.06, 0.06, 0.0]^T$
6	$[2.0, 1.5, 0.0]^T$	$[0.06, 0.06, 0.0]^T$
7	$[2.0, -1.5, 0.0]^T$	$[0.06, -0.06, 0.0]^T$
8	$[-2.0, -1.5, 0.0]^T$	$[-0.06, -0.06, 0.0]^T$

4.1 Geometric cable span

In Fig. 4 the cable span is visualized in polar coordinates. The points in the plot indicate the unfiltered data (258 vertices) received from the workspace evaluation. The circumferential red line is drawn from the 36 vertices received from polar sorting.

In order to assess the computational performance, the same computation was executed with a higher number of vertices. The computation time for the cable span of all eight cables for 16 386 vertices on the workspace hull was determined to be 51 ms (on Intel Core i5-5200U at 2.2 GHz) while the workspace determination consumed some 1050 ms of CPU time. Thus, the determination of the cable span is cheap in terms of computation efforts.

4.2 Deflection angles for anchor points

Another application of the cable span lies in the dimensioning of the panning pulley unit on the machine frame of the robot. This supports the mechanical design of the cable robot when the initial position of the cable guiding system needs to be defined. Using the computation of the cable span, one maps the extremal values with the pulley kinematics function [11].

Fig. 5 and Fig. 6 show the actually occurring deflection angles $\beta_{k,1}$ and $\gamma_{k,1}$ in the pulley mechanism for the IPAnema 1 robot. The sample poses are chosen from the hull of the workspace thus covering the extremal positions of the pulley. One can see that the panning angle γ_k of the pulley is in the range $[-\frac{\pi}{2}; 0]$ thus pointing to the inside of the machine frame. The considered winch $i = 1$ is an upper winch located at the top of the robot frame. Thus, the wrapping angle is $\beta_{k,1} \in [\frac{\pi}{2}; \pi]$ where the cable always wraps at least a quarter of the pulley. Only a small part of the toroidal surface is actually used. The region where the point C_i may be located is notably smaller than the torus.

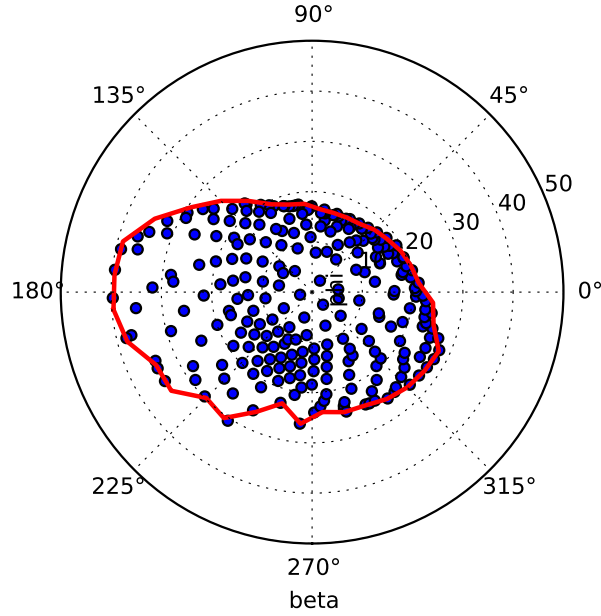


Fig. 4 Plot of the cable span in polar coordinates of frame $\mathcal{K}_{A,1}$

A similar consideration is applied to the platform. If we consider only the translational workspace, the deflection angles on the platform are essentially the same as for the proximal anchor point but with inverted sign (see Fig. 2). For the distal anchor point B_i , two mechanical constructions are widespread, the use of universal/spherical joints at the end of the cable and swivel bolts (see Fig. 7). Their main difference lies in the admissible deflection of the cable with respect to the installation orientation. For universal and spherical joints, the preferred attack angle is within a cone where an attack angle of 0° is optimal. This installation orientation of the joint shall thus be aligned with the central axis of the cable span for proper operation and the deflection angles shall lie inside the cable span. In contrast, swivel bolts allow for very large deflection angles which can even exceed 90° . However, the swivel bolt has a singular configuration when the direction of the cable and the first axis of the swivel bolt is aligned. Therefore, a sufficient diagonal pull on the swivel bolt must be guaranteed (see Fig. 7). In this setting, the generalized cone computed from the cable span must be placed within the range of γ_{\min} and γ_{\max} .

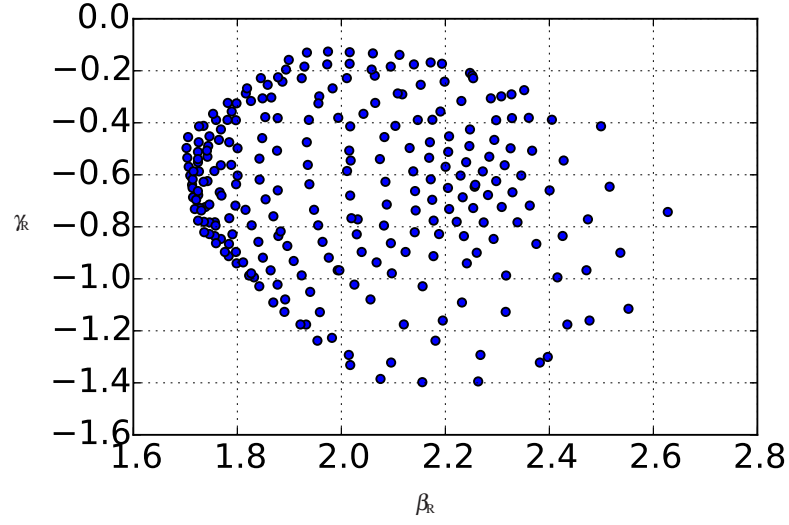


Fig. 5 Deflection angles β_k and γ_k for the first winches of the IPAnema 1 robot throughout the workspace.

5 Conclusion

In this paper, the concept cable span is introduced and an efficient algorithm for the determination of the region occupied by the cables is presented. As the geo-

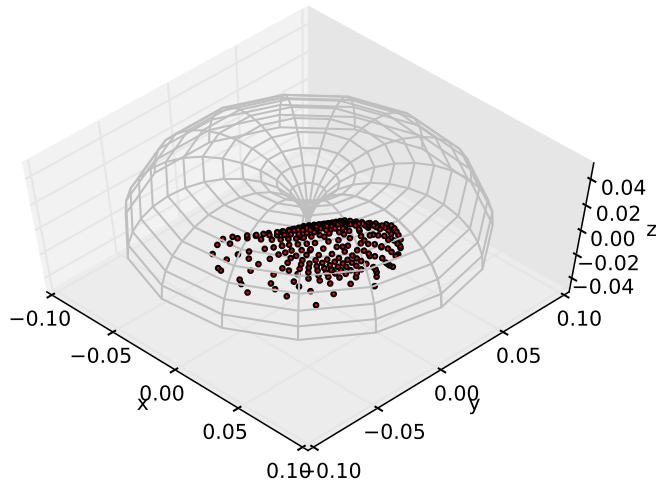


Fig. 6 Actual proximal anchor points C_1 where the cable leaves the pulley in the local frame $\mathcal{H}_{A,1}$

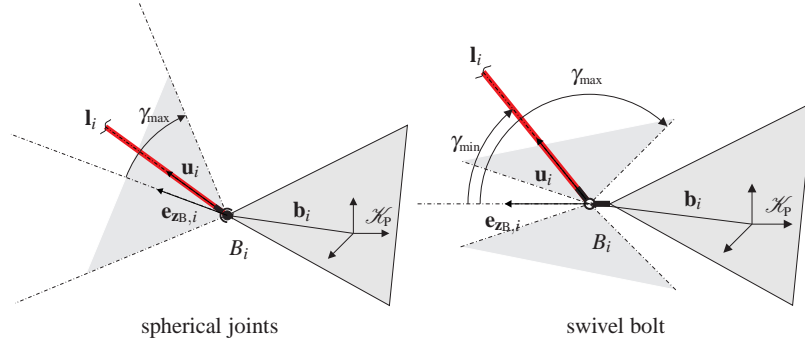


Fig. 7 Feasible deflection angles (gray area left of the platform) for the cable on the platform for spherical joints and swivel bolts

metric structure of the cable span is a generalized cone, it can be represented as a triangulation of its shell surface. This object can be used in CAD planning to study interference with other equipment. Furthermore, the cable span is a useful concept to design the cable guiding system in order to choose feasible orientation value for the axis of the pulleys.

Acknowledgements The authors would like to thank the German Research Foundation (DFG) for financial support of the project within the Cluster of Excellence in Simulation Technology (EXC 310/1) at the University of Stuttgart.

References

1. Bouchard, S., Moore, B., Gosselin, C.: On the ability of a cable-driven robot to generate a prescribed set of wrenches. *Journal of Mechanisms and Robotics* **2**(1), 1–10 (2010).
2. Ebert-Uphoff, I., Voglewede, P.A.: On the Connections Between Cable-Driven Parallel Manipulators and Grasping. In: *IEEE International Conference on Robotics and Automation*, 2004, pp. 4521–4526. New Orleans (2004)
3. Ghasemi, A., Farid, M., Eghesad, M.: Interference free workspace analysis of redundant 3D cable robots. In: *World Automation Congress*, 2008, pp. 1–6 (2008).
4. Gouttefarde, M., Gosselin, C.: On the properties and the determination of the wrench-closure workspace of planar parallel cable-driven mechanisms. *Proceedings of the ASME Design Engineering Technical Conference* **2**, 337–346 (2004).
5. Lamaury, J., Gouttefarde, M.: Control of a large redundantly actuated cable-suspended parallel robot. In: *IEEE International Conference on Robotics and Automation*, 2013, pp. 4659–4664 (2013).
6. Maeda, K., Tadokoro, S., Takamori, T., Hiller, M., Verhoeven, R.: On design of a redundant wire-driven parallel robot WARP manipulator. In: *Proceedings of IEEE International Conference on Robotics and Automation*, 1999, pp. 895–900. Detroit, MI, USA (1999)
7. Merlet, J.P.: Analysis of the Influence of Wires Interference on the Workspace of Wire Robots. In: *Advances in Robot Kinematics (ARK)*, pp. 211–218. Kluwer Academic Publishers, Sestri Levante, Italy (2004)

8. Miermeister, P., Lächele, M., Boss, R., Masone, C., Schenk, C., Tesch, J., Kerger, M., Teufel, H., Pott, A., Bühlhoff, H.: The CableRobot Simulator: Large Scale Motion Platform Based on Cable Robot Technology. In: IEEE/RSJ International Conference on Intelligent Robots and Systems, Daejeon, South Korea (2016)
9. Perreault, S., Cardou, P., Gosselin, C., Otis, M.J.D.: Geometric determination of the interference-free constant-orientation workspace of parallel cable-driven mechanisms. *ASME Journal of Mechanisms and Robotics* **2**(3) (2010).
10. Pott, A.: Forward Kinematics and Workspace Determination of a Wire Robot for Industrial Applications. In: *Advances in Robot Kinematics (ARK)*, pp. 451–458. Springer (2008)
11. Pott, A.: Influence of Pulley Kinematics on Cable-Driven Parallel Robots. In: *Advances in Robot Kinematics (ARK)*, pp. 197–204 (2012)
12. Pott, A., Bruckmann, T., Mikelsons, L.: Closed-form Force Distribution for Parallel Wire Robots. In: *Computational Kinematics*, pp. 25–34. Springer, Berlin, Heidelberg (2009)
13. Pott, A., Mütherich, H., Kraus, W., Schmidt, V., Miermeister, P., Verl, A.: IPAnema: A family of Cable-Driven Parallel Robots for Industrial Applications. In: *Cable-Driven Parallel Robots, Mechanisms and Machine Science*, pp. 119–134. Springer (2012)
14. Verhoeven, R.: Analysis of the Workspace of Tendon-based Stewart Platforms. PhD thesis, University of Duisburg-Essen, Duisburg, Germany (2004)
15. Verhoeven, R., Hiller, M.: Estimating the Controllable Workspace of Tendon-Based Stewart Platforms. In: *Advances in Robot Kinematics (ARK)*, pp. 277–284. Springer, Portorož, Slovenia (2000)